

Tumor targeting in photodynamic therapy. From glycoconjugated photosensitizers to glycodendrimeric one. Concept, design and properties

S everine Ballut,^{a,b,c,d} Ali Makky,^{d,e,f} Beno t Chauvin,^{a,b,c,d,g} Jean-Philippe Michel,^{d,e,f} Athena Kasselouri,^{d,g} Philippe Maillard^{*a,b,c,d} and V eronique Rosilio^{d,e,f}

Received 24th January 2012, Accepted 17th April 2012

DOI: 10.1039/c2ob25181g

In this paper, we discuss the evolution over the last 15 years in the Curie Institute of the concept, the development of the design and some properties of glycoconjugated photosensitizers with the aim to optimize the tumor targeting in photodynamic therapy. By this research, we have shown that specific interactions between a mannose-lectin and trimannosylglycodendrimeric porphyrins contributed to a larger extent than non-specific ones to the overall interaction of a glycosylated tetraarylporphyrin with a membrane. The studies of *in vitro* photocytotoxicity showed the relevance of the global geometry of the photosensitizer, the number and position of the linked glycopyranosyl groups on the chromophore and their lipophilicity. The two best compounds appeared to be porphyrins bearing three α -glycosyl groups on *para*-position of *meso*-phenyl *via* a flexible linker. Compound bearing α -mannosyl moieties was evaluated successfully in two *in vivo* xenografted animal models of human retinoblastoma and colorectal cancers. Conversely, the presence on the chromophore of three sugars *via* a glycodendrimeric moiety induced a potential cluster effect, but decreased the *in vitro* photoefficiency despite a good affinity for a mannose-lectin.

Introduction

The incorporation of carbohydrates on photosensitizers usable in photodynamic therapy (PDT) continues to be pursued vigorously by a number of research teams, particularly during these last two years.^{1–3} In these systems, glycoconjugation is considered to be a potentially effective way to increase their water solubility by modifying the amphiphilicity of macrocycles. Moreover, it provides the possibility of specific interaction of the resulting conjugates with lectin-type receptors overexpressed in some types of malignant cells. It is expected that coupling multivalent carbohydrates to the porphyrin core allows their interaction with more than one receptor binding site at the same time and increases their affinity, resulting in better cellular recognition and uptake. Pandey's team of Roswell Park Cancer Institute at Buffalo have shown that the uptake of glycoconjugated photosensitizers

involve sugar membrane receptors such as galectins 1 and 3 and the overexpressed ABCG2 transporter in RIF and Colon26 cells.^{1,d,2b,4,5} S. Hirohara *et al.* evaluated the cellular uptake of the glycoconjugated chlorins in HeLa cells. All glycoconjugated chlorins showed higher cellular uptake than the hydrosoluble tetraphenylporphyrin tetrasulfonic acid.⁶ Recently, Hocine *et al.* have shown that a functionalization with mannose of photosensibilizing nanoparticles was necessary to obtain the best results with PDT due to an active endocytosis mediated by a membrane receptor.⁷

Dendrimers are an ideal delivery vehicle candidate for explicit study of the effects of polymer size, charge, composition, and architecture on biologically relevant properties such as lipid bilayer interactions, cytotoxicity, internalization, blood plasma retention time, biodistribution, and tumour uptake. Over the last several years, substantial progress has been made towards the use of dendrimers for therapeutic and diagnostic purposes for the treatment of cancer, including advances in the delivery of anti-neoplastic and contrast agents, neutron capture therapy, photodynamic therapy, and photothermal therapy.⁸

In recent years, several articles and reviews describing the utility of porphyrin-based compounds in photodynamic therapy were published.⁹ In one of our laboratories† efforts have been

^aInstitut Curie, Centre de Recherche, B at 110-112, Orsay, F-91405, France

^bCNRS, UMR 176, Centre Universitaire, Orsay, F-91405, France

^cUniv Paris-Sud 11, Centre Universitaire, Orsay, F-91405, France

^dCNRS GDR 3049 PHOTOMED, UMR 5623, Universit  Paul Sabatier, F-31062 Toulouse, cedex 9, France. E-mail: philippe.maillard@curie.u-psud.fr; Fax: +(33) 01 6907 5327; Tel: +33 01 6986 3171

^eCNRS, UMR 8612, F-92296 Ch tenay-Malabry, France

^fUniv Paris-Sud 11, UMR 8612, Laboratoire de Physico-chimie des Surfaces, IFR 141, 5 rue Jean-Baptiste Cl ment, F-92296 Ch tenay-Malabry cedex, France

^gUniv Paris-Sud 11, EA 4041, Laboratoire de Chimie Analytique, IFR 141, F-92296 Ch tenay-Malabry, France

†Institut Curie, Centre de Recherche, B at 110-112, Orsay, F-91405, France; CNRS, UMR 176, Centre Universitaire, Orsay, F-91405, France; Univ Paris-Sud 11, Centre Universitaire, Orsay, F-91405, France.

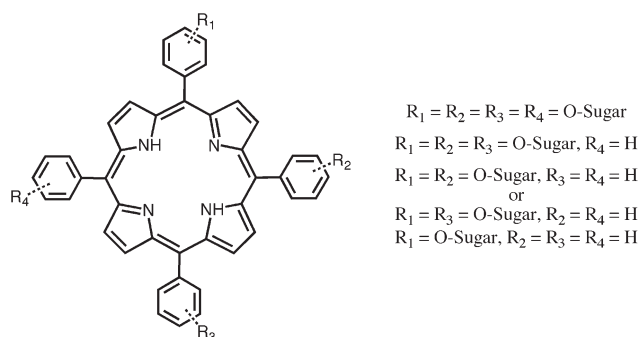


Fig. 1 Glycoconjugated photosensitizers with a constrained structure.

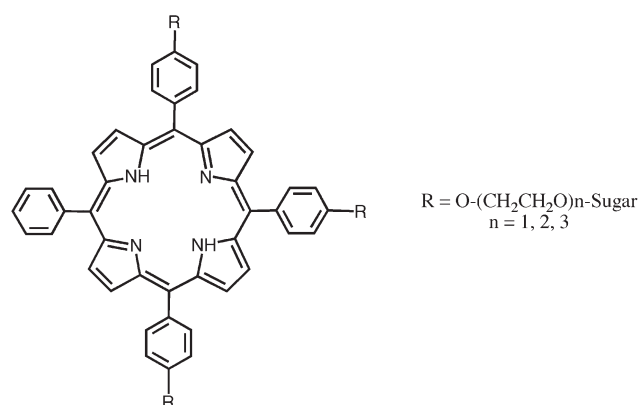


Fig. 2 Glycoconjugated photosensitizers with a flexible structure.

focused on the preparation, *in vitro* and *in vivo* evaluation of the phototoxicity of a broad series of neutral targeted tetrapyrrolic macrocycles as potential photosensitizing agents for photodynamic therapy. The targeting was obtained by glycoconjugation.¹⁰ Three types of glycoconjugated photosensitizers were investigated differentiated by the nature of connection between the macrocycle and the sugar. In the first one, sugar was linked directly on the phenyl group of a tetraphenyl porphyrin by an ether function which, in the case of *ortho*- and *meta*-position substitution, induced a constrained structure (Fig. 1).

A second family of glycoconjugated porphyrins was prepared with the aim of exploring the effect on the *in vitro* phototoxicity of incorporation of the extended and more flexible diethylene glycol linker between the chromophore and glycosyl moieties (Fig. 2). The third one relied on a glycodendrimeric structure for inducing a potential increase of tumour targeting by a cluster effect (Fig. 3).

In this paper, we discuss the respective imperfections and advantages of every strategy.

Synthesis

Constrained photosensibilizing macromolecules

Synthesis of the *meso*-tetraarylporphyrins bearing glycosylated moieties on phenyl groups required the condensation of pyrrole and miscellaneous *ortho*, *meta* or *para*-glycosylated benzaldehyde restricted only to the β -saccharides,¹¹ under Lindsey's conditions¹² in yield between 10 and 26%.¹³ shown in Fig. 4.

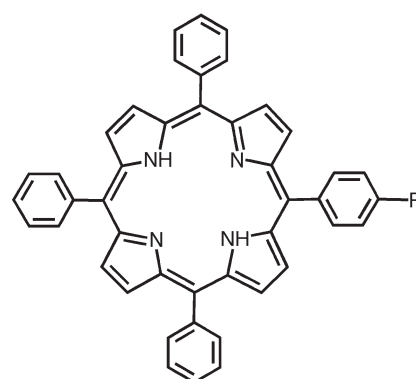


Fig. 3 Glycodendrimeric photosensitizers.

However, many trials have been performed in an attempt to link a glycoside directly to porphyrin *via* the ether link without success. In order to obtain mono-, bis-, and tris(tetraacetyl-sugar-phenyl)-tri-, bis- and mono-phenyl porphyrins, pyrrole in methylene chloride was condensed with a mixture of benzaldehyde and *ortho*, *meta* and *para*-(2,3,4,6-tetraacetyl-O- β -D-glycosyl)benzaldehyde in relative proportions of 4/2/2, under the same conditions, in total yield near 30%. Optimised conditions with relative proportions of 4/1/3 of pyrrole, benzaldehyde and glycosylated benzaldehyde respectively were used for the preparation of tri-glycosylated porphyrins.

Flexible glycoconjugated photosensitizers

All flexible glycosylated photosensitizers were prepared from 5,10,15-(tri-*para*-phenol)-20-phenylporphyrin by a modified Williamson's protocol in DMF in the presence of cesium carbonate in range 20–50% yield, as shown in Fig. 5. This strategy allowed to prepare α - and β -compounds with a variable length for the linker between the sugar and the macrocycle.¹⁴

Glycodendrimeric photosensitizing agents

It would be advantageous to use the transport mechanisms through biological membranes for a photosensitizer targeting tumour cells. In this context, the use of glycodendrimers as recognition motifs seems very exciting. Carbohydrate–protein interactions play a crucial role in a large number of biological processes.¹⁵ Due to the weak nature – in the millimolar range – of interactions between a single specific carbohydrate and a receptor protein subunit, nature uses cluster carbohydrates in order to obtain biologically meaningful affinities for the receptors. The cluster effect appears when several carbohydrates interact with more than one receptor binding site simultaneously and cooperatively, resulting in better cellular recognition.^{16,17} Lectin receptors are multisubunits and multivalent proteins with many important biological functions. Dendritic structures (glycodendrimers) are emerging as effective ligands for

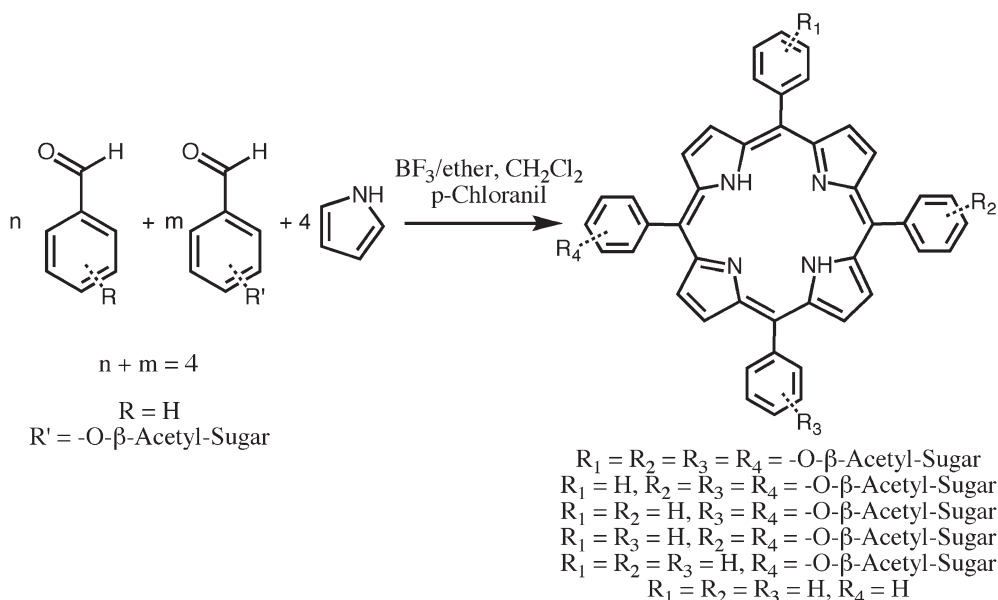


Fig. 4 Synthesis of constrained glycosylated porphyrins.

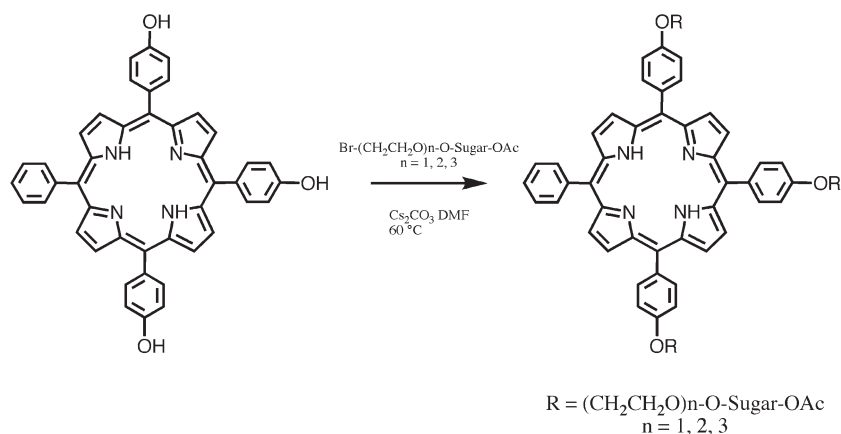


Fig. 5 Synthesis of flexible glycosylated photosensitizers.

carbohydrate-binding proteins.¹⁸ In very recent papers,^{10a,10d} we have described the design and synthesis of new glycoconjugated photosensitizers bearing a glycodendrimeric group in the vicinity of the chromophore. In the structure of glycodendrimeric compounds shown in Fig. 3 and 6, the presence of $\text{-CH}_2\text{CH}_2\text{CONH-}$ ($\text{CH}_2\text{CH}_2\text{O}$) _{n} -, $\text{-CH}_2\text{CH}_2\text{-CONH-}$ ($\text{CH}_2\text{CH}_2\text{O}$)₂-, or $\text{-CH}_2\text{CH}_2\text{CONH-}$ ($\text{CH}_2\text{CH}_2\text{O}$)₃- linkers between amino acid (glycyl or L-phenylalanyl) and glycoside parts reduces steric constraints between sugars and induces some variable flexibility of the sugars. The presence of an amino acid could lead to a modification of the hydrophobic contribution of dendrimeric moieties, which could change the cellular uptake of photosensitizer or its anchorage in the lipid membrane of the targeted cancer cell.

All glycoconjugated porphyrins bearing free glycosyl were obtained in quantitative yield from acetylated compounds by trans-esterification described by Zemlén *et al.* in 1936.¹⁹

Spectroscopic properties

NMR

The NMR spectra of glycosylated porphyrins are governed by the symmetry properties of the products. On the other hand, the general aspects of the ¹H NMR spectra of constrained *ortho*-O-glycosylated porphyrins (Fig. 7) are similar to those of the both-faces hindered porphyrins previously studied.²⁰

For example, the ¹H NMR spectra of the atropoisomers $\alpha,\beta,\alpha,\beta$, $\alpha,\alpha,\beta,\beta$ and $\alpha,\alpha,\alpha,\beta$, which have, respectively, D₂, C₂ and C₁ symmetries, should be differentiated from each other. The spectra of the isomer $\alpha,\beta,\alpha,\beta$ is relatively simple, each resonance system corresponding to four equivalent protons while for compound $\alpha,\alpha,\beta,\beta$ they appear as two distinct resonances of two chemically equivalent protons. Each proton of the isomer $\alpha,\alpha,\alpha,\beta$ has its own resonance. Steric considerations suggest that

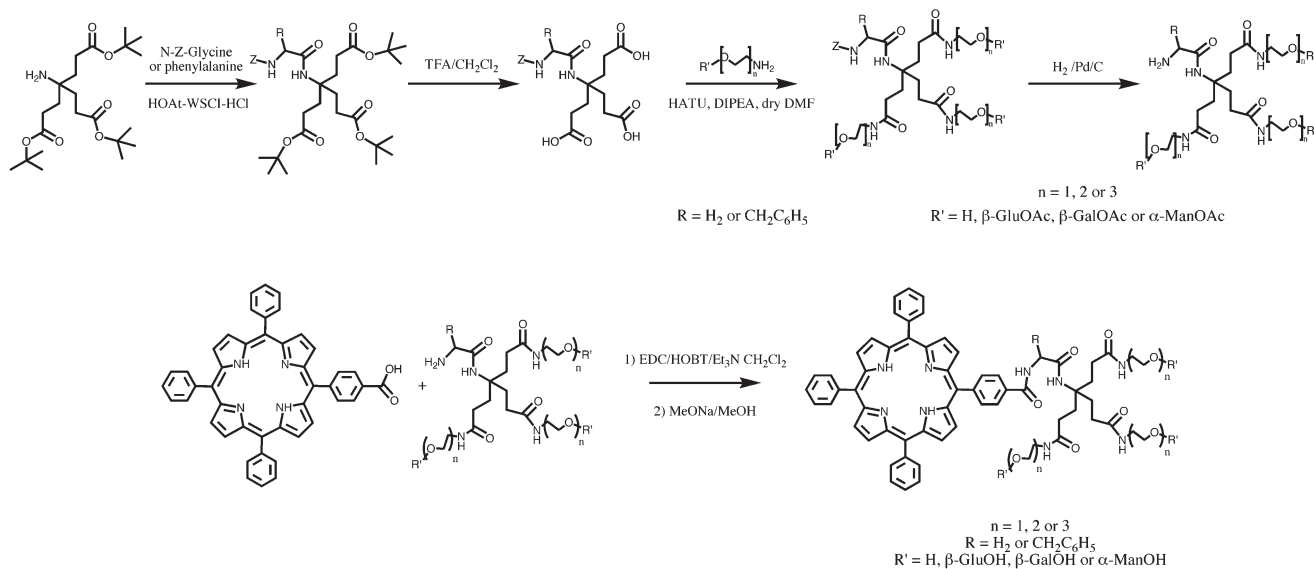


Fig. 6 Synthesis of flexible glycodendrimeric photosensitizers.

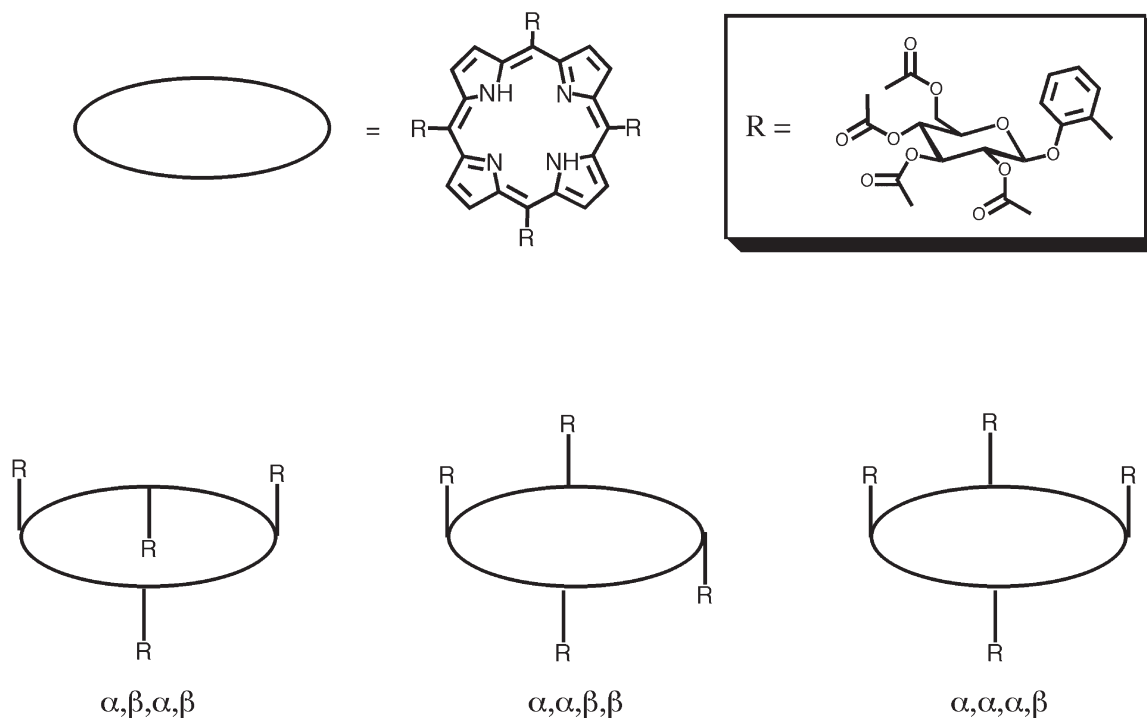


Fig. 7 Structure of constrained *ortho*-O-glucosylated porphyrins.

all sugar groups should be oriented in the same direction with C-2 and C-3 sugar protons towards the center of the macrocycle. For $\alpha, \beta, \alpha, \beta$, $\alpha, \alpha, \beta, \beta$ and $\alpha, \alpha, \alpha, \beta$ compounds, resonances of the glycosyl protons are shifted upfield between 0.1 and 1.3 ppm with respect to the resonance of the same protons in the protected helicin taken as reference. At the same time the methyl protons of the acetyl groups are shifted up to 4.3 ppm, which suggests that the *meso* substituents of these compounds bend over the porphyrin ring in spite of the spatial congestion. The effect of temperature on the number of NH resonances in the ^1H NMR spectra of these compounds showed an intense

tautomerism effect observed near room temperature, which could be explained by the motional restriction resulting from a very high steric hindrance due to acetylglucosyl groups.¹³ Such an effect has been described by other groups with similar molecules.²¹ Furthermore, the ^1H NMR resonances of anomeric proton of the protected and unprotected constrained *ortho*, *meta* and *para*-O-glycosylated-porphyrins appear as a well-defined doublet ($J = 8$ Hz) between 4.80 and 5.30 ppm in CDCl_3 and 5.60 and 5.80 ppm in deuterated pyridine. This indicates a pure β -configuration of the anomeric carbon of the sugars.²² The general aspect of the ^1H NMR spectra of the *para*-glycosylated

porphyrins (flexible, and glycodendrimeric ones) is similar to that of the *ortho*-glycosylated porphyrins except for the acetyl resonances of saccharide moieties, which are not shifted downfield. This shows that the glycosylated substituents are not affected by the ring current of the macrocycle. The absence of the deshielding effects is consistent with a conformation of compounds in which the glycosylated substituents are located in the same plane of the porphyrin ring. Because of the D_{2h} symmetry of *meso*-tetra(*para*-O-glycosyloxyaryl)porphyrins, the resonances of the eight equivalent pyrrolic protons appear as single peaks at 8.80 ppm. The ^1H NMR spectra of flexible glycosylated and glycodendrimeric compounds are composed of five main groups of resonance: the pyrrolic protons appearing near 8.85 ppm as one singlet (6H) and one doublet (2H), the phenyl protons as complex signals between 8.31 and 7.75 ppm, the sugar protons between 5.18 and 3.66 ppm, protective acetyl group protons between 2.16 and 1.97 ppm, and NH protons near -2.8 ppm. The anomeric proton resonance of the flexible glycosylated and glycodendrimeric photosensitizers appears as a well-defined doublet with $J = 8\text{--}9$ Hz (characteristic of a β anomeric configuration for glucosyl and β -galactosyl derivatives), and as a narrow doublet with $J < 2$ Hz (α anomeric configuration) for the mannosylated and α -galactosylated compound.^{10,14}

UV-visible and fluorescence spectra and aggregation

Electronic absorption spectra of glycoconjugated photosensitizers (Fig. 1–3) in organic media present the well-known optical characteristics of *meso*-tetraarylporphyrins derivatives:²³ four bands between 500 and 650 nm (Q_{Y10} , Q_{Y00} , Q_{X10} , Q_{X00} bands) and one very intense ($\epsilon \sim 400$ L mmol^{-1} cm^{-1}) around 420 nm (Soret band or B band). Glycoconjugation at *para* positions of the phenyl groups induces slight red shifts in both B and Q bands. Substitution at *meta* position results in both blue and red shifts depending on considered bands.²⁴ Band shifts increase with the electrodonating character and the number of the substituents. The observed differences are limited: band shifts do not exceed 3–4 nm with respect to the bands of unsubstituted *meso*-tetraarylporphyrin. Fluorescence emission spectra present one main band (Q^*_{X00}) around 650 nm and a second one of lower intensity (Q^*_{X01}) around 720 nm. Emission maxima only slightly shift with glycoconjugation (3–4 nm), contrary to the relative intensity of the two bands, which highly depends on the position (*ortho*, *meta* or *para*) of the substituent. Fluorescence emission yield is low for all derivatives, between 0.05 and 0.07.^{24,25} Electronic (absorption and emission) spectra vary only slightly with the nature of the organic solvent.²⁶ As only minor differences exist in spectra characteristics, all compounds can be excited and detected in solution or *in vivo* using the same apparatus.

Electronic absorption spectra of photosensitizers vary with pH. Indeed, *meso*-tetraarylporphyrins should undergo protonation of both nitrogens located at the core of the tetrapyrrole macrocycle, a basic character enhanced by electrodonating character of substituents. However, even for most basic compounds, that is *para*-tetraglycoconjugated derivatives, protonation could be neglected in neutral conditions, such as biological media described below.²⁷ Free base *meso*-tetraarylporphyrins are highly

hydrophobic, and thus insoluble in aqueous media. The effect of sugar residues on the overall hydrophobicity of the tetraphenylporphyrin has been evaluated chromatographically.²⁸ Besides polarity heightens with increasing number of substituents, results have shown that flexible structures are more hydrophobic than constrained structures and *para* derivatives are more polar than their *meta* isomers. Although glycoconjugation increases photosensitizer polarity, its solubility in water remains very low and photosensitizer molecules (Fig. 1–3) aggregate in aqueous media. The nature and extent of aggregates are very sensitive to photosensitizer structure and conformation. They are a function of (i) the number and (ii) position of sugars, (iii) the presence of a spacer or (iv) existence of a dendrimeric configuration. Since the aggregation process induces significant modifications in both the absorption and fluorescence spectra, porphyrin aggregation phenomena are commonly studied by electronic spectroscopy. Sharp Soret bands in phosphate buffer are only reported for some polar tetraglycoconjugated photosensitizers described in Fig. 1.^{25,29} Aggregate formation depends on the position (*ortho*, *meta*, *para*) of sugars, which influences photosensitizer conformation. However, in all cases a decrease in molar absorptivity is reported with respect to the spectra in methanol. Soret bands for triglycoconjugated derivatives are larger and lower than those for the corresponding tetraglycoconjugated ones.^{24,25} Modifications of electronic spectra (decrease in absorptivity and band broadening) are found to be even more pronounced for the photosensitizers in Fig. 2 and 3 that present flexible bulky substituents, with a splitting of the Soret band into two bands of low intensity.²⁴ Red and blue shifts observed upon aggregation could be respectively associated with two different relative positions of tetrapyrroles in the aggregate: side by side (type-J aggregates) or face to face (type-H aggregates).³⁰ Aggregation is almost always accompanied by a significant decrease in fluorescence emission yield.

Analytical applications

Study of photosensitizers – biomolecules interactions

Photosensitizer aggregation is expected to take place in biological media, as the process is favoured in an aqueous environment. Nevertheless, it has been demonstrated that in solution the presence of biomolecules such as albumin, or phospholipid (PL) liposomes, induces progressive dissociation of glycoconjugated porphyrin aggregates; the photosensitizer binds to biomolecules in its monomer form.²⁹ The difference in spectroscopic characteristics between the aggregates and the monomer (especially the difference in emission intensity) is a powerful analytical tool for revealing photosensitizer–biomolecule interactions. The association of some of the glycoconjugated photosensitizers (Fig. 1–3) with dimyristoylphosphatidylcholine (DMPC) liposomes has been studied by absorption, steady state and time-resolved fluorescence spectroscopy, fluorescence anisotropy and fluorescence quenching. Photosensitizer–biomolecule association is rapid at 37 °C for the constrained tri- and tetraglycoconjugated photosensitizers. The association is stronger for the asymmetric tri-substituted compound than for the symmetric tetraglycoconjugated one.²⁹ For some *para*-tetraglycoconjugated derivatives, no association to liposomes could be detected.^{25,29,31}

Triglycoconjugated compounds with a flexible structure (Fig. 2) and glycodendrimeric photosensitizers (Fig. 3) present slow kinetics association (6–8 h) and intermediate affinity for liposomes.²⁹ The depth of penetration into a phospholipid bilayer is directly related to the number of free phenyl groups and is particularly high for the glycodendrimeric compounds in Fig. 3. The introduction of a spacer between the phenyl and the sugar increases the depth of penetration: flexible triglycoconjugated compounds (Fig. 2) are inserted deeper in the bilayer than the triglycoconjugated one with a constrained structure (Fig. 1). Tetraglycoconjugated photosensitizers that have no free phenyl remain in the polar region of a phospholipid bilayer.^{25,29} Besides the effect on fluorescence intensity described above, aggregation deeply affects the shape of fluorescence spectra (broadness and relative intensity of the two bands). This explains that considering the whole spectra through a multiwavelength analysis improves monitoring of monomerization upon interactions with biomolecules. This kind of approach has been recently applied to study interactions of glycoconjugated photosensitizers with plasma proteins (albumin and lipoproteins).²⁴ Even if glycoconjugated tetraphenylporphyrins strongly bind to plasma proteins, plasma distribution studies have underlined the central role of high density lipoproteins. A flexible structure favors interactions with lipoproteins when compared with more constrained *para*-triglycoconjugated derivatives. In a similar way, fluorescence should be applied to the study of the interactions of porphyrins with other compounds than biomolecules, as for example with cyclodextrin, a potential delivery agent.³²

Detection and quantitation

High absorptivity and natural fluorescence emission of porphyrin derivatives have been extensively used for photosensitizer detection and quantitation in biological media. Fluorimetric detection is more selective and more sensitive than absorption, and optimized protocols have been developed for photosensitizer quantitation in plasma, tissues or cell suspensions. The photosensitizer is quantified by direct measurement of the fluorescence emission of the extract, or after coupling with high performance liquid chromatography.³³ The developed protocols have allowed determination of the pharmacokinetics of glycoconjugated PS,^{34,35} their uptake and metabolization in cells.¹⁴

Interactions with membrane models

Glycosylated and hydroxylated *meso*-tetraarylporphyrins do not penetrate into cancerous cells through the same pathway.¹⁴ For the former, a protein exposed at the cell membrane surface, possibly a lectin, would facilitate their penetration into the cell, whereas for the latter penetration would be mainly controlled by passive diffusion. The evaluation of a glycosylated porphyrin interaction with phospholipids (PLs) and lectins can thus be used as a screening method to anticipate drug effectiveness.

The interaction of various glycosylated *meso*-tetraarylporphyrins with phospholipids forming Langmuir films and liposomes has been first studied, with the aim to identify the physicochemical parameters involved in the passive mechanism of intracellular penetration of these photosensitizers. Surface tension and

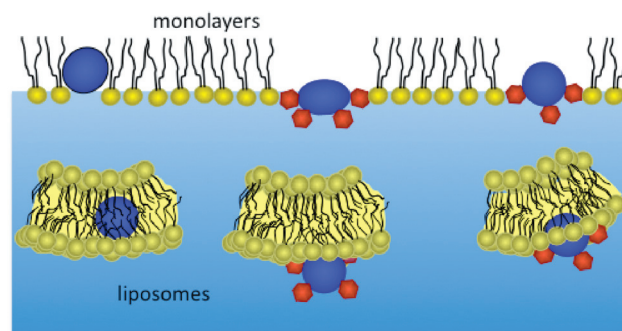


Fig. 8 Organization of *meso*-tetraarylporphyrins in lipid monolayers and liposome bilayers.

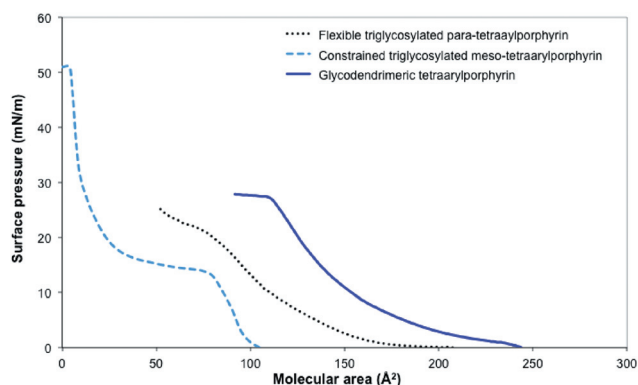


Fig. 9 Interfacial behaviour of the triglycosylated porphyrin derivatives.

surface pressure measurements, grazing incidence X-ray diffraction, liquid chromatography on an IAM stationary phase and fluorescence spectroscopy experiments have revealed that a hydroxylated *meso*-tetraarylporphyrin could interact with the studied phospholipids and significantly disorganize the structure of their monolayers. A constrained triglycosylated *meso*-tetraarylporphyrin also interacted with the PL, though to a lesser extent. Conversely, the tetraglycosylated derivative exhibited both a weak surface activity and a poor affinity for the studied phospholipids. A model of the organization of the constrained tetraphenylporphyrin derivatives in mixtures with PL could be drawn from this study (Fig. 8).³⁴

The flexible triglycosylated *para*-tetraarylporphyrin (Fig. 2), in which the phenyl groups are separated from the sugar moieties by a diethylene oxide spacer, has shown a different interfacial organization than that of the constrained triglycosylated *meso*-tetraarylporphyrin (Fig. 9). It occupied a larger molecular area, and was not solubilized upon compression. The immersion of its spacers and sugar moieties into the subphase considerably lowered its collapse surface pressure. It could not be embedded in the membrane of liposomes, but its interaction with PL vesicles could be studied by fluorescence spectroscopy, which showed at first a weak affinity to PLs. However, when porphyrin concentration was lowered, its apparent affinity increased. This would account for the role of the monomer/dimer equilibrium in porphyrin solutions. Indeed, the flexible triglycosylated *para*-tetraarylporphyrin has a stronger tendency to self-associate in

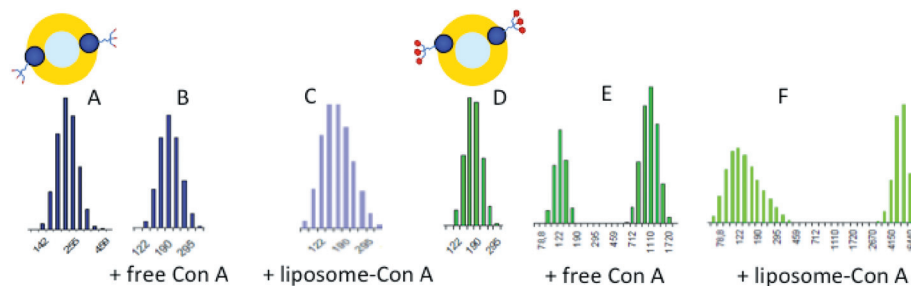


Fig. 10 Effect of lectin–sugar interaction on lipid vesicles size. Vesicles bearing non-glycosylated porphyrin (A) or glycosylated porphyrin (D) in the presence of free Con A (B, E) or Con A-grafted liposomes (C, F).

solution than the constrained triglycosylated derivative. Concentration lowering would favour the dissociation of aggregates and porphyrin penetration into phospholipid vesicle membranes.²⁹

The most interesting results have been achieved with dendrimeric porphyrins (Fig. 3). Indeed, due to the additional flexibility and amphipathy conferred by the dendron, these molecules could be more easily studied by interfacial measurement techniques. When injected into a water phase at a very low concentration, dendrimeric porphyrins adsorbed at the interface. Their surface properties were enhanced by the presence of sugars moieties and by longer spacers.³⁶ Their non-specific interaction with a membrane was first modelled using the monolayer approach. The composition of a complex mixed monolayer was chosen to fit the description of healthy and pathological retinal cell membranes, as described in the literature.³⁷ Hybrid PLs with both stearyl (S) and oleoyl (O) chains were used, varying in the structure of the polar head groups. Phosphatidylethanolamine (PE) and phosphatidylcholine (PC) molar fractions were varied between 0.35 and 0.45, while the phosphatidylserine (PS) one was kept constant at 0.1 from one model to another. Cholesterol (CHOL) was added to the mixtures at a molar fraction between 0 and 0.3. When the dendrimeric porphyrins were injected beneath a SOPC/SOPE/SOPS/CHOL monolayer, surface pressure increments could be monitored up to initial surface pressures of 28 and 35 mN m⁻¹ for the non-glycosylated and the mannosylated dendrimeric porphyrin with the same spacer length, respectively. The profile of the surface pressure changes *versus* initial surface pressure indicated an adsorption–penetration mechanism. Dendrimeric porphyrins were added to liposome suspensions to determine the partition coefficient and the depth of their penetration into the membrane by fluorescence spectroscopy. The results confirmed that the cholesterol rate in a membrane had no influence on porphyrin partition into liposomes. The penetration depth analysed by fluorescence quenching with potassium iodide showed that the non-glycosylated porphyrin penetrated to a slightly higher extent into the phospholipid bilayer than the glycodendrimeric porphyrins.³⁶ All dendrimeric porphyrins could form stable monolayers by spreading from volatile organic solutions at the air/water interface (Fig. 9). Due to their good surface properties and favourable interactions with PLs, they could be incorporated into dimyristoylphosphatidylcholine (DMPC) liposome bilayers, which allowed studying more particularly their interaction with a lectin modelling the mannose receptor of retinoblastoma cells.^{10d} Indeed, since the tetrapyrrolic cycle was embedded into the liposome bilayer, non-specific hydrophobic interactions were reduced, and only sugar–lectin

Table 1 Quartz crystal frequency (ΔF) shifts measured upon interaction of porphyrin derivatives with pure Con A and Con A-grafted supported lipid bilayer (DP: non-glycosylated porphyrin, GDP 1: glycosylated dendrimeric porphyrin with a 2 ethylene oxide unit spacer, GDP 2: glycosylated dendrimeric porphyrin with a 3 ethylene oxide unit spacer)

Nature of the sensor layer	ΔF (Hz)			
	Vesicles	Vesicles-DP	Vesicles-GDP 1	Vesicles-GDP 2
Pure Con A	-17	-21	-130	-186
Con A-grafted bilayer	-5	-5	-72	-72
Lipid bilayer	-5	-5	-5	-5

interactions could take place. Porphyrin-bearing vesicles were first mixed with free concanavalin A (Con A). The interaction was evaluated by dynamic light scattering. There was no change in size or distribution of vesicles in which the non-glycosylated porphyrin had been incorporated. Conversely, for glycodendrimeric porphyrins, the addition of free Con A led to bimodal size distribution. The longer the spacer, the larger aggregate size. When Con A was grafted to model liposomes (SOPC-SOPE-SOPS-CHOL) and these liposomes were mixed to vesicles bearing the porphyrins, the effect on the size of vesicles was even more dramatic, due to liposomes bridging (Fig. 10). Again the interaction was stronger for the glycodendrimeric porphyrin having the longest spacer.³⁸

In order to assess the specific interaction when mobility of the lectin was strongly reduced, as is the case for a membrane receptor, Con A has been grafted onto the sensor surface of a quartz crystal microbalance (QCM-D) and porphyrin-bearing liposomes have been subsequently injected into the aqueous flow. The specific interaction was confirmed by the significant change in crystal resonance frequency and energy dissipation, as was the favourable influence of the spacer (Table 1).³⁹ After rinsing, injection of methyl- α -D-mannopyranoside (α -MMP), a competitor for Con A binding, provoked an increase in frequency shift indicating the replacement of porphyrin-bearing vesicles by α -MMP molecules. Finally, to fully mimic the cell membrane, with the lipids and receptor, a SOPC/DOPE/SOPS/CHOL bilayer was formed by liposome breaking onto the sensor of a QCM and Con A was grafted *in situ*. After rinsing, DMPC liposomes bearing the dendrimeric porphyrins were injected under flow into the measurement cell (Fig. 11).

Porphyrin free liposomes and those incorporating the non-mannosylated dendrimeric porphyrin did not produce any

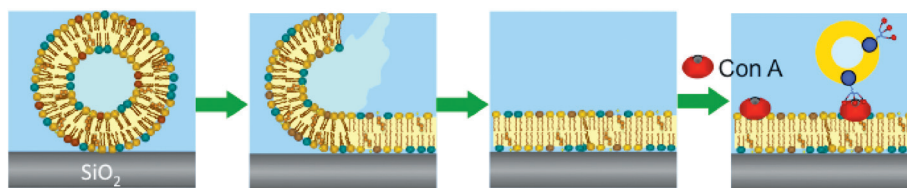


Fig. 11 Formation of a lipid-Con A bilayer and interaction with glycodendrimeric porphyrin-bearing vesicles (from ref. 39).

significant change in the frequency shift and energy dissipation of the sensor. They adsorbed at the surface and were removed by rinsing. Conversely, for liposomes bearing the mannosylated dendrimeric porphyrins, significant decrease in frequency shift and increase in energy dissipation were observed. They were stronger for the porphyrin having the longest spacer (Table 1). The decrease in frequency shift indicated the adsorption of vesicles and the increase in dissipation, a more viscous behaviour of the whole system. Liposomes were adsorbed and could not be removed following rinsing, accounting for the strong interaction between the glycosylated dendrimeric porphyrins and the lectin. When the glycodendrimeric porphyrin-bearing liposomes were injected into a measurement cell containing a Con A free bilayer, no adsorption occurred.³⁹ This confirmed that, in our experiments, the lectin–sugar interaction was the sole mechanism affecting the QCM-D signal.

In general, our results showed that specific interactions contributed to a larger extent than non-specific ones to the overall interaction of a glycosylated dendrimeric tetraarylporphyrin with a membrane. The chemical structure of the porphyrin derivatives appeared to be crucial in controlling this interaction.

Photobiological results: cellular phototoxicity

Phototoxicity of the photosensitizer was determined in HT29 and Y79 cells lines by cell survival fraction measurements after incubation for 24 hours (Table 2) and exposure to red light >540 nm with a fluence of 1.8 J cm⁻². Toxicity in darkness was found to be negligible in all cases, with a survival fraction close to 100% (2 μM, 4 h or 24 h incubation). It is important to mention that under the same experimental conditions (data not shown), Foscan® was cytotoxic in the dark for Y79 cells with a 50% cell survival fraction for treated cells (2 μM, 4 h incubation). The results are presented in Table 2.

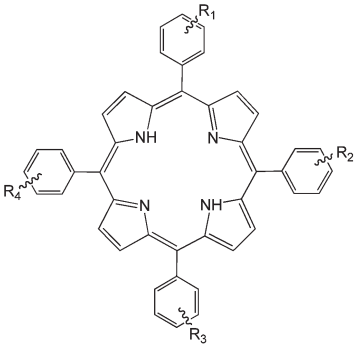
Nonglycoconjugated photosensitizers (R₁ = R₂ = R₃ = R₄ = p-OH or R₁ = R₂ = R₃ = p-OH, R₄ = H) appeared weakly photo-efficient (IC₅₀ between 2.2 and 0.5 μM), and for R₁ = R₂ = R₃ = p-O-Deg-OH, R₄ = H or R₁ = -CONH-Gly-CONH-C(CH₂CH₂CONH-Deg-OH)₃, R₂ = R₃ = R₄ = H, the photoefficiency was even weaker (IC₅₀ > 2 μM). The tetraglycoconjugated compounds (*ortho*, *meta* and *para*-O-β-D-Glucose) did not show any phototoxicity (IC₅₀ > 10 μM) against HT29 cell line, and were weakly efficient against the Y79 cell one (IC₅₀ between 1.5 and 2.6 μM). The glycoconjugated derivatives bearing three α-glycopyranosyl groups as D-galactose and D-mannose linked by a diethylene glycol to *meso*-phenyl substituents (IC₅₀ = 0.1 and 0.4 μM, 0.05 and 0.35 μM against HT29 and Y79 respectively) were more phototoxic than β-glycopyranosyl ones (O-D-glucosyl: IC₅₀ = 1.2 and 0.5 μM, and O-D-galactosyl: 0.7 and

0.6 μM against HT29 and Y79 respectively). These results showed the pertinence of glycopyranosyl groups for a good efficiency of photodynamic effect. Despite a potential cluster effect, the presence of one glycodendrimeric moiety containing three α- or β-glycopyranosyl groups, linked to a *meso*-phenyl, decreases the photocytotoxicity of photosensitizers.

In vivo phototoxicity

In a previous paper, we have shown that the PDT using first and second generation of photosensitizers (Photofrin® and Foscan®) could be efficient *in vivo* against retinoblastoma.⁴⁰ Among the glycoconjugated photosensitizers presented in this paper, one (Table 2, compound with R₁ = R₂ = R₃ = p-O-Deg-O-α-mannose and R₄ = H) which was very efficient in *in vitro* tests and that showed some retinoblastoma (Y79) and colorectal (HT29) cell affinity, was used on retinoblastoma and colorectal animal models. These models were obtained by xenografted retinoblastoma or colorectal human tumors provided by the Transfer Department of Curie Institute.^{40,41} Two tumors were implanted subcutaneously on the flank of nude mice; only one side was illuminated by laser light (653 nm) whereas the other side was used as an un-illuminated reference. The longitudinal follow-up of the tumors was carried out by ²³Na MRI (without adding exogenous contrast agents) to map the extracellular compartment and to characterize cell packing. Two regimens based on pharmacokinetic studies³⁵ were used to target either blood vessels alone or blood vessels and cancer cells simultaneously.^{35,41} The first one targeting only blood vessel consists of one single intravenous injection of photosensitizer (0.6 mg kg⁻¹) followed 10 min later by exposure to light. In a second protocol targeting both cancer cells and blood vessels, one intravenous dose of mannosyl-porphyrin was followed by a second half dose, separated by a 3 h interval, then the tumor area was illuminated after 10 min. Tumor volume evolution was followed by ²³Na/¹H MRI examinations. For example, retinoblastoma (a) and colorectal (b) tumor volume evolutions are shown in Fig. 12.

In the two animal models, a single anti-vasculature PDT protocol did not induce an important necrose or/and apoptose of the tumor. In the case of colorectal tumor, anti-vasculature PDT protocol had a immediate effect on the blood vessel but the tumor volume increased until the end of experiments (10 days) [Fig. 12 (b)]. Only the double-targeting regimen (blood vessel and tumor) gave an important regression of tumors more than those obtained with the non-glycoconjugated photosensitizers such as Photofrin® and Foscan®. In the case of retinoblastoma tumors, the tumor progression stopped after three days [Fig. 12(a)] and steadied over the following 10 days.

Table 2 Phototoxicity of compounds on HT29 and Y79 cell lines after incubation (24 h) and illumination with red light (1.8 J cm^{-2} , $\lambda > 540 \text{ nm}$)


$R_1^{a,b,c,d}$	R_2	R_3	R_4	$\log P \pm 0.3$	HT29, IC_{50}^f	Y79, IC_{50}^f
<i>o</i> -O-D- β -Glucose	<i>o</i> -O- β -D-Glucose	<i>o</i> -O-D-Glucose	<i>o</i> -O-D-Glucose		>10	—
<i>m</i> -O-D- β -Glucose	<i>m</i> -O- β -D-Glucose	<i>m</i> -O-D-Glucose	<i>m</i> -O-D-Glucose		>10	1.5
<i>p</i> -OH <i>p</i> -O-D- β -Glucose	<i>p</i> -OH <i>p</i> -O- β -D-Glucose	<i>p</i> -OH <i>p</i> -O-D-Glucose	<i>p</i> -OH <i>p</i> -O-D-Glucose	0.3	2.2 >10	2 2.6
<i>p</i> -OH <i>p</i> -O-D- β -Glucose	<i>p</i> -OH <i>p</i> -O- β -D-Glucose	<i>p</i> -OH <i>p</i> -O-D-Glucose	H		0.5	0.8
<i>p</i> -O-Deg-OH	<i>p</i> -O-Deg-OH	<i>p</i> -O-Deg-OH	H	1.2	1.3	0.9
<i>p</i> -O-Deg-O- β -Glucose ^a	<i>p</i> -O-Deg-O- β -D-Glucose	<i>p</i> -O-Deg-O- β -D-Glucose	H	>2 nd	nd 1.2	>2 0.5
<i>p</i> -O-Deg-O- β -Galactose	<i>p</i> -O-Deg-O- β -D-Galactose	<i>p</i> -O-Deg-O- β -D-Galactose	H	-0.07	0.7	0.6
<i>p</i> -O-Deg-O- α -Galactose	<i>p</i> -O-Deg-O- α -D-Galactose	<i>p</i> -O-Deg-O- α -D-Galactose	H	0.5	0.1	0.05
<i>p</i> -O-Deg-O- α -Mannose	<i>p</i> -O-Deg-O- α -D-Mannose	<i>p</i> -O-Deg-O- α -D-Mannose	H	1	0.4	0.35
-CONH-Gly-CONH-C(CH ₂ CH ₂ CONH-Deg-OH) ₃ ^b	H	H	H	1.6	5	6
-CONH-Gly-CONH-C(CH ₂ CH ₂ CONH-Meg-O- β -D-Glucose) ₃ ^c	H	H	H	-0.5	2.	3.7
-CONH-Gly-CONH-C(CH ₂ CH ₂ CONH-Deg-O- β -D-Glucose) ₃	H	H	H	-0.8	5	>10
-CONH-Gly-CONH-C(CH ₂ CH ₂ CONH-Meg-O- β -D-Galactose) ₃	H	H	H	-0.7	3	5
-CONH-Gly-CONH-C(CH ₂ CH ₂ CONH-Deg-O- β -D-Galactose) ₃	H	H	H	-0.9	2.5	3
-CONH-Gly-CONH-C(CH ₂ CH ₂ CONH-Meg-O- α -D-Mannose) ₃	H	H	H	-0.6	2.7	3.7
-CONH-Gly-CONH-C(CH ₂ CH ₂ CONH-Deg-O- α -D-Mannose) ₃	H	H	H	-0.65	5	5.6
-CONH-Gly-CONH-C(CH ₂ CH ₂ CONH-Teg-O- α -D-Mannose) ₃ ^d	H	H	H	-0.95	5	5
-CONH-Phen-CONH-C(CH ₂ CH ₂ CONH-Meg-O- β -D-Glucose) ₃ ^e	H	H	H	-0.7	4.5	5
-CONH-Phen-CONH-C(CH ₂ CH ₂ CONH-Deg-O- β -D-Glucose) ₃	H	H	H	-1	6	>10
-CONH-Phen-CONH-C(CH ₂ CH ₂ CONH-Meg-O- β -D-Galactose) ₃	H	H	H	-0.7	4	5
-CONH-Phen-CONH-C(CH ₂ CH ₂ CONH-Deg-O- β -D-Galactose) ₃	H	H	H	-1	>10	>10
-CONH-Phen-CONH-C(CH ₂ CH ₂ CONH-Meg-O- α -D-Mannose) ₃	H	H	H	-0.6	3.7	5.2
-CONH-Phen-CONH-C(CH ₂ CH ₂ CONH-Deg-O- α -D-Mannose) ₃	H	H	H	-0.3	4.4	6

^a Deg = CH₂CH₂O-CH₂CH₂-. ^b Gly = glycyl group. ^c Meg = CH₂CH₂-. ^d Teg = CH₂CH₂O-CH₂CH₂-O-CH₂CH₂-. ^e Phen = L-phenylalanyl group. ^f In μM .

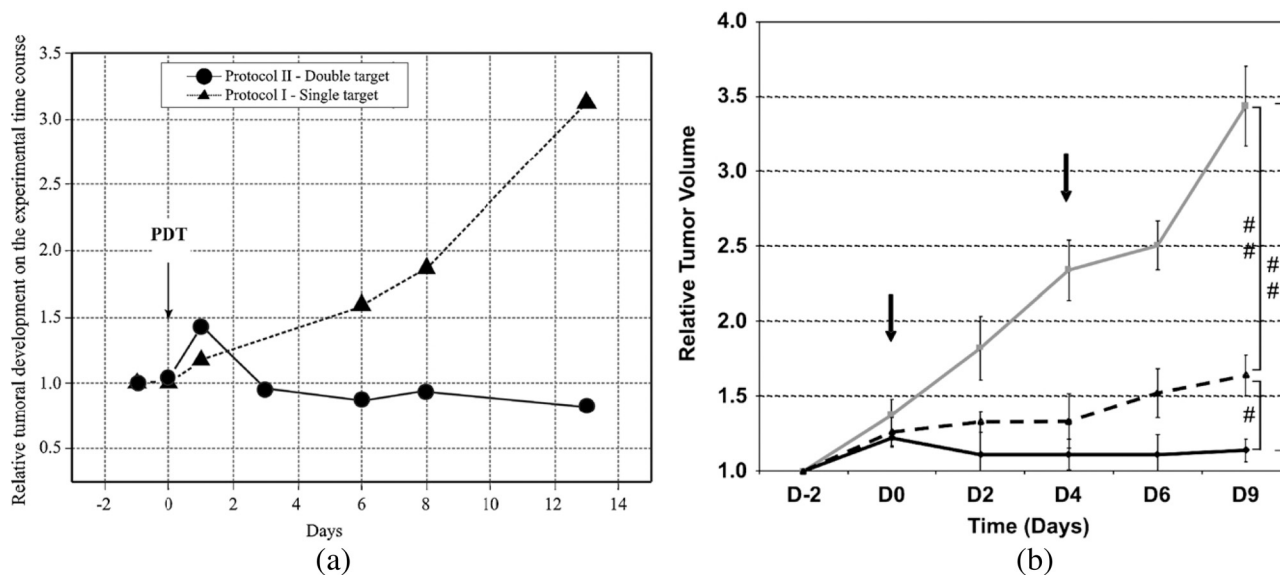


Fig. 12 (a) Retinoblastoma tumor volumes as determined from the ^1H -images, are plotted as a function of time. The single-dose anti-vascular protocol led finally to a 3-fold increase of the tumor volume (\blacktriangle). The double-targeting protocol slightly decreased the tumor volume (\bullet). Both treatments were monitored over the same time length (2 weeks). From ref. 35. (b) Colorectal tumor volume evolution (relative representation) for all PDT protocols: grey, controls; ---, antivasular PDT; —, double-targeting PDT. The arrows indicate the treatment days. Only double-targeted PDT succeeded in stopping the tumor growth, # $p < 0.05$, ## $p < 0.01$. (At day -2, the tumor dimensions were not statistically different between the groups: $266 \text{ mm}^3 \pm 31$ for the SC group, $272 \text{ mm}^3 \pm 39$ for the DC group and $202 \text{ mm}^3 \pm 17$ for the control group.) From ref. 41.

Conclusion

The chemistry used in this work allowed the synthesis of several families of pure globular or flat glycoconjugated photosensitizers bearing three and four β - and α -glycopyranosyl moieties *via* rigid ether, flexible polyethylene glycol and glycodendrimeric linkers on the *meso*-phenyl group of *meso*-(5,10,15,20-tetraaryl) porphyrins. These compounds were all characterized by spectroscopic techniques such as proton and ^{13}C NMR, UV-visible, fluorescence spectra and aggregation properties. The results obtained from fluorescence spectroscopy have allowed study of the interactions of the glycoconjugated porphyrins with some biomolecules like albumin and phospholipids. High absorptivity and fluorescence emission of glycoconjugated derivatives have been used for photosensitizer detection and quantitation in biological media. Fluorimetric detection appears more selective and more sensitive than absorption, and optimized protocols have been developed for photosensitizer quantitation in plasma, tissues or cell suspensions. The studies of glycoconjugated photosensitizer's interactions with membrane models such as Langmuir films and modified liposomes have allowed for the first time identification of the physicochemical parameters involved in the passive or active mechanism of intracellular penetration. Our results have shown that specific interactions between a mannose-lectin and tri-mannosylglycodendrimeric porphyrins contributed to a larger extent than non-specific ones to the overall interaction of a glycosylated tetraarylporphyrin with a membrane. The chemical structure of the porphyrin derivatives appeared to be crucial in controlling this interaction. The studies of *in vitro* photocytotoxicity in two tumour cell lines (HT29 and Y79) showed the relevance of the global geometry of the photosensitizer, the number and position of the linked glycopyranosyl groups on the chromophore, and the hydrophobicity

of the molecule. The two best compounds appeared to be porphyrins bearing three α -glycosyl groups on *para*-position of *meso*-phenyl *via* a flexible linker. Conversely, the presence on the chromophore of three sugars *via* a glycodendrimeric moiety inducing a potential cluster effect, decreased the *in vitro* photoefficiency despite a good affinity for a mannose-lectin. We showed that the glycosylation of photosensitizers notably increases the *in vivo* photodynamic activity on two animal models (retinoblastoma and colorectal xenografted tumors on nude mice) compared with results obtained with Photofrin® and Foscan®.

To further progress in PDT, particularly for *in vivo* applications, targeted two-photon excitation (TPE) will be developed. TPE exploits the high penetration of IR radiation (750–1000 nm) in tissues coupled with high three-dimensional spatial resolution. Thus TPE-PDT will be particularly indicated for focal therapy of small solid tumours.⁴²

Acknowledgements

The authors acknowledge CNRS, the "Programme Incitatif et Coopératif Rétinoblastome" of Institut Curie, and the nonprofit French organization "Rétinostop" (www.retinostop.org) for their financial support. B. Chauvin has benefited from a "Postes d'accueil CNRS-CEA-APHP" grant and A. Makky of a PhD grant from ARC (Association for Cancer Research).

References

- (a) R. Vallinayagam, F. Schmitt, J. Barge, G. Wagnières, V. Wenger, R. Neier and L. Juillerat-Jeanneret, *Bioconjugate Chem.*, 2008, **19**, 821; (b) S. Hirohara, M. Obata, H. Alitomo, K. Sharyo, S.-I. Ogata, C. Ohtsuki, S. Yano, T. Ando and M. Tanihara, *Biol. Pharm. Bull.*, 2008,

- 31, 2265; (c) C.-F. Choi, J.-D. Huang, P.-C. Lo, W.-P. Fong and D. K. P. Ng, *Org. Biomol. Chem.*, 2008, **6**, 2173; (d) X. Zheng and R. K. Pandey, *Anti-Cancer Agents Med. Chem.*, 2008, **8**, 241.
- 2 (a) Y. Zorlu, M. A. Ermeýdan, F. Dumoulin, V. Ahsen, H. Savoie and R. W. Boyle, *Photochem. Photobiol. Sci.*, 2009, **8**, 312; (b) X. Zheng, J. Morgan, S. K. Pandey, Y. Chen, E. Tracy, H. Baumann, J. R. Missert, C. Batt, J. Jackson, D. A. Bellnier, B. W. Henderson and R. K. Pandey, *J. Med. Chem.*, 2009, **52**, 4306; (c) A. R. M. Soares, J. P. C. Tomé, M. G. P. M. S. Neves, A. C. Tomé, J. A. S. Cavaleiro and T. Torres, *Carbohydr. Res.*, 2009, **344**, 507; (d) F. Ménard, V. Sol, C. Ringot, R. Granet, S. Alves, C. Le Morvan, Y. Queneau, N. Ono and P. Krausz, *Bioorg. Biomol. Chem.*, 2009, **17**, 7647; (e) J. R. McCarthy, J. Bhaumik, N. Merbouh and R. Weissleder, *Org. Biomol. Chem.*, 2009, **7**, 3430; (f) J.-Y. Liu, P.-C. Lo, W.-P. Fong and D. K. P. Ng, *Org. Biomol. Chem.*, 2009, **7**, 1583; (g) Z. Iqbal, M. Hanack and T. Ziegler, *Tetrahedron Lett.*, 2009, **50**, 873; (h) Z. Iqbal, A. Lyubimtsev, M. Hanack and T. Ziegler, *Tetrahedron Lett.*, 2009, **50**, 5681; (i) S. Hirohara, M. Obata, H. Alitomo, K. Sharyo, T. Ando, S. Yano and M. Tanihara, *Bioconjugate Chem.*, 2009, **20**, 944; (j) S. Hirohara, S. M. Obata, H. Alitomo, K. Sharyo, T. Ando, M. Tanihara and S. Yano, *J. Photochem. Photobiol., B*, 2009, **97**, 22.
- 3 (a) E. Hao, T. J. Jensen and M. G. H. Vicente, *J. Porphyrins Phthalocyanines*, 2009, **13**, 51; (b) M. A. Grin, I. S. Lonin, A. A. Lakhina, E. S. Ol'shanskaya, A. L. Makarov, Y. L. Sebyakin, L. Guryeva, P. V. Toukach, A. S. Kononikhin, V. A. Kuzminc and A. F. Mironov, *J. Porphyrins Phthalocyanines*, 2009, **13**, 336; (c) A. T. P. C. Gomes, R. A. C. Leão, F. C. da Silva, M. G. P. M. S. Neves, M. A. F. Faustinoa, A. C. Tomé, A. M. S. Silva, S. Pinheiro, M. C. B. V. de Souza, V. F. Ferreira and J. A. S. Cavaleiro, *J. Porphyrins Phthalocyanines*, 2009, **13**, 247; (d) M. B. Bakar, M. Oelgemöller and M. O. Senge, *Tetrahedron*, 2009, **65**, 7064.
- 4 S. K. Pandey, X. Zheng, J. Morgan, J. R. Missert, T.-H. Liu, M. Shibata, D. A. Bellnier, A. R. Oseroff, B. W. Henderson, T. J. Dougherty and R. K. Pandey, *Mol. Pharmaceutics*, 2007, **4**, 448.
- 5 W. Liu, M. R. Baer, M. Bowman, P. Pera, X. Zheng, J. Morgan, R. K. Pandey and A. R. Oseroff, *Clin. Cancer Res.*, 2007, **13**, 2463.
- 6 S. Hirohara, M. Obata, S.-I. Ogata, C. Ohtsuki, S. Higashida, S.-I. Ogura, I. Okura, M. Takenaka, H. Ono, Y. Sugai, Y. Mikata, M. Tanihara, Y. Masao and S. Yano, *J. Photochem. Photobiol., B*, 2005, **78**, 7–15.
- 7 (a) O. Hocine, M. Gary-Bobo, D. Brevet, M. Maynadier, S. Fontanel, L. Raehm, S. Richeter, B. Looock, P. Couleaud, C. Frochot, C. Charnay, G. Derrien, M. Smâihî, A. Sahmoune, A. Morère, Ph. Maillard, M. Garcia and J.-O. Durand, *Int. J. Pharm.*, 2010, **402**, 221; (b) O. Hocine, M. Gary-Bobo, D. Brevet, M. Maynadier, L. Raehm, S. Richeter, B. Looock, A. Morère, Ph. Maillard, M. Garcia and J.-O. Durand, *Int. J. Pharm.*, 2012, **423**, 509.
- 8 J. B. Wolinsky and M. W. Grinstaff, *Adv. Drug Delivery Rev.*, 2008, **60**, 1037.
- 9 (a) M. Ethirajan, Y. Chen, P. Joshi and R. K. Pandey, *Chem. Soc. Rev.*, 2011, **40**, 340; (b) A. M. Bugaj, *Photochem. Photobiol. Sci.*, 2011, **10**, 1097; (c) A. Robertson, D. Hawkins Evans and H. Abrahamse, *J. Photochem. Photobiol., B*, 2009, **96**, 1.
- 10 (a) S. Ballut, D. Naud-Martin, B. Looock and Ph. Maillard, *J. Org. Chem.*, 2011, **76**, 2010; (b) G. Garcia, D. Naud-Martin, D. Carrez, A. Croisy and Ph. Maillard, *Tetrahedron*, 2011, **67**, 4924; (c) S. Achelle, P. Couleaud, P. Baldeck, M.-P. Teulade-Fichou and Ph. Maillard, *Eur. J. Org. Chem.*, 2011, 1271; (d) S. Ballut, A. Makky, B. Looock, J.-Ph. Michel, Ph. Maillard and V. Rosilio, *Chem. Commun.*, 2009, 224.
- 11 S. Halazy, V. Berges, A. Ehrhard and C. Danzin, *Bioorg. Chem.*, 1990, **18**, 330.
- 12 (a) J. S. Lindsey, in *Metalloporphyrins Catalyzed Oxidations*, ed. F. Montanari and L. Casella, Kluwer Academic Publishers, Netherlands, 1994, p. 49; (b) A. W. Van der Made, E. J. H. Hoppenbrouwer, R. J. Nolte and W. Drenth, *Recl. Trav. Chim. Pays-Bas*, 1988, **107**, 15; (c) J. S. Lindsey, I. C. Schreiman, H. C. Hsu, P. C. Kearney and A. M. Marguerettaz, *J. Org. Chem.*, 1987, **52**, 827; (d) R. W. Wagner, D. S. Lawrence and J. S. Lindsey, *Tetrahedron Lett.*, 1987, **28**, 3069; (e) J. S. Lindsey, H. C. Hsu and I. C. Schreiman, *Tetrahedron Lett.*, 1986, **22**, 931.
- 13 (a) D. Oulmi, Ph. Maillard, J.-L. Guerquin-Kern, C. Huel and M. Momenteau, *J. Org. Chem.*, 1995, **60**, 1554; (b) Ph. Maillard, J.-L. Guerquin-Kern, C. Huel and M. Momenteau, *J. Org. Chem.*, 1993, **58**, 2774; (c) Ph. Maillard, J.-L. Guerquin-Kern, M. Momenteau and S. Gaspard, *J. Am. Chem. Soc.*, 1989, **111**, 9125.
- 14 I. Laville, S. Pigaglio, J.-C. Blais, F. Doz, B. Looock, Ph. Maillard, D. S. Grierson and J. Blais, *J. Med. Chem.*, 2006, **49**, 2558.
- 15 (a) A. Varki, *Glycobiology*, 1993, **3**, 97; (b) L. Wells, K. Vosseller and G. W. Hart, *Science*, 2001, **291**, 2376; (c) P. M. Rudd, T. Elliott, P. Cresswell, I. A. Wilson and R. A. Dwek, *Science*, 2001, **291**, 2370.
- 16 (a) L. L. Kiessling and N. L. Pohl, *Chem. Biol.*, 1996, **3**, 71; (b) M. Mammen, S.-K. Choi and G. M. Whitesides, *Angew. Chem., Int. Ed.*, 1998, **37**, 2754; (c) L. L. Kiessling, J. E. Gestwicki and L. E. Strong, *Curr. Opin. Chem. Biol.*, 2000, **4**, 696; (d) T. K. Lindhorst, *Top. Curr. Chem.*, 2001, **218**, 201.
- 17 M. Monsigny, R. Mayer and A.-C. Roche, *Carbohydr. Lett.*, 2000, **4**, 35.
- 18 (a) R. Roy, *Curr. Opin. Struct. Biol.*, 1996, **6**, 692; (b) T. K. Lindhorst and C. Kieburg, *Angew. Chem., Int. Ed. Engl.*, 1996, **35**, 1953.
- 19 G. Zemplén, A. Gerecs and C. Hadácsy, *Ber.*, 1936, **69**, 1827.
- 20 M. Momenteau, J. Mispelter, B. Looock and J.-M. Lhoste, *J. Chem. Soc., Perkin Trans. 1*, 1985, 61.
- 21 (a) Y. Kuroda, T. Hiroshige, T. Sera, Y. Shirowa, H. Tanaka and H. Ogoshi, *J. Am. Chem. Soc.*, 1989, **111**, 1912; (b) R. J. Abraham, G. E. Hawkes, M. F. Hudson and K. M. Smith, *J. Chem. Soc., Perkin Trans. 2*, 1975, 205.
- 22 A. F. Casy, *PMR Spectroscopy in Medicinal and Biological Chemistry*, Academic Press, London and New York, 1971, p. 330.
- 23 H. N. Fonda, J. V. Gilbert, R. A. Cormier, J. R. Sprague, K. Kamioka and J. S. Connolly, *J. Phys. Chem.*, 1993, **97**, 7024.
- 24 B. Chauvin, PhD thesis, Université Paris-sud 11, 2011.
- 25 G. Csik, E. Balog, I. Voszka, F. Tölgyesi, D. Oulmi, Ph. Maillard and M. Momenteau, *J. Photochem. Photobiol., B*, 1998, **44**, 216.
- 26 H. Ibrahim, A. Kasselouri, B. Raynal, R. Pansu and P. Prognon, *J. Lumin.*, 2011, **131**, 2528.
- 27 B. Chauvin, A. Kasselouri, P. Chaminade, R. Quiameso, I. Nicolis, Ph. Maillard and P. Prognon, *Anal. Chim. Acta*, 2011, **705**, 306.
- 28 K. Valko, C. Bevan and D. Reynolds, *Anal. Chem.*, 1997, **69**, 2022.
- 29 H. Ibrahim, A. Kasselouri, C. You, Ph. Maillard, V. Rosilio, R. Pansu and P. Prognon, *J. Photochem. Photobiol., A*, 2011, **217**, 10.
- 30 N. C. Maiti, S. Mazumdar and N. Periasamy, *J. Phys. Chem. B*, 1998, **102**, 1528.
- 31 I. Voszka, R. Galantai, Ph. Maillard and G. Csik, *J. Photochem. Photobiol., B*, 1999, **52**, 92.
- 32 A. Bautista-Sanchez, A. Kasselouri, M.-C. Desroches, J. Blais, Ph. Maillard, D. Manfrim de Oliveira, A. C. Tedesco, P. Prognon and J. Delaire, *J. Photochem. Photobiol., B*, 2005, **81**, 154.
- 33 F. Cañada-Cañada, A. Bautista-Sánchez, M. Taverna, P. Prognon, Ph. Maillard, D. S. Grierson and A. Kasselouri, *J. Chromatogr., B: Anal. Technol. Biomed. Life Sci.*, 2005, **821**, 166.
- 34 M.-C. Desroches, A. Bautista-Sanchez, C. Lamotte, B. Labeque, D. Auchère, R. Farinotti, Ph. Maillard, D. S. Grierson, P. Prognon and A. Kasselouri, *J. Photochem. Photobiol., B*, 2006, **85**, 56.
- 35 M. Lupu, C. D. Thomas, Ph. Maillard, B. Looock, B. Chauvin, I. Aerts, A. Croisy, E. Belloir, A. Volk and J. Mispelter, *Photodiagn. Photodyn. Ther.*, 2009, **6**, 214.
- 36 A. Makky, J. P. Michel, S. Ballut, A. Kasselouri, Ph. Maillard and V. Rosilio, *Langmuir*, 2010, **26**, 11145.
- 37 (a) A. J. Fliesler and R. E. Anderson, *Prog. Lipid Res.*, 1983, **22**, 79; (b) D. Huster, K. Arnold and K. Gawrisch, *Biochemistry*, 1998, **37**, 17299; (c) D. Huster, K. Arnold and K. Gawrisch, *Biophys. J.*, 2000, **78**, 3011.
- 38 A. Makky, J. P. Michel, A. Kasselouri, E. Briand, Ph. Maillard and V. Rosilio, *Langmuir*, 2010, **26**, 12761.
- 39 A. Makky, J. P. Michel, Ph. Maillard and V. Rosilio, *Biochim. Biophys. Acta, Biomembr.*, 2011, **1808**, 656.
- 40 I. Aerts, P. Leuraud, J. Blais, A.-L. Pouliquen, Ph. Maillard, C. Houdayer, J. Couturier, X. Sastre-Garau, F. Doz and M.-F. Poupon, *Photodiagn. Photodyn. Ther.*, 2010, **7**, 275–283.
- 41 F. Poyer, C. D. Thomas, G. Garcia, A. Croisy, D. Carrez, Ph. Maillard, M. Lupu and J. Mispelter, *Photodiagn. Photodyn. Ther.*, 2012, DOI: 10.1016/j.pdpdt.2012.03.001.
- 42 (a) S. Achelle, P. Couleaud, M.-P. Teulade-Fichou and Ph. Maillard, *Eur. J. Org. Chem.*, 2011, 1271; (b) S. Achelle, N. Saettel, P. Baldeck, M.-P. Teulade-Fichou and Ph. Maillard, *J. Porphyrins Phthalocyanines*, 2011, **14**, 877; (c) F. Hammerer, S. Achelle, P. Baldeck, Ph. Maillard and M.-P. Teulade-Fichou, *J. Phys. Chem. A*, 2011, **115**, 6503.